Osmotic compression and expansion of highly ordered dispersions

Céline Martin, Frédéric Pignon, Albert Magnin, Martine Meireles, Vincent Lelièvre, Peter Lindner, Bernard Cabane

La052605k(250) “Osmotic compression and expansion of highly ordered clay dispersions”

Table of Contents Graphics

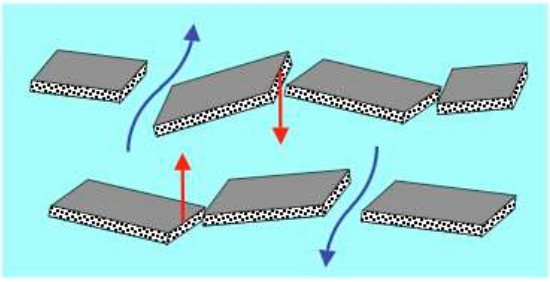

Osmotic compression and expansion of highly ordered clay dispersions

Céline Martin[1], Frédéric Pignon[1], Albert Magnin[1], Martine Meireles[2], Vincent Lelièvre[1,2], Peter Lindner[3], Bernard Cabane[4]*

1 Laboratoire de Rhéologie, Université Joseph Fourier, Grenoble I, Institut National Polytechnique de Grenoble, CNRS UMR 5520, BP 53, 38041 Grenoble Cedex 9, France

2 Laboratoire de Génie Chimique, CNRS UMR 5503, Université Paul Sabatier, 118 Route de Narbonne, 31062 Toulouse Cedex 4, France

3 Institut Laue-Langevin, B.P. 156, 38042 Grenoble Cedex 9, France

4 Laboratoire de Physique et Mécanique des Milieux Hétérogènes, CNRS UMR 7636, ESPCI, 75231Paris Cedex 05, France

* Author to whom correspondence should be addressed. E-mail: bcabane@pmmh.espci.f

Abstract

Aqueous dispersions of nanometric clay platelets (Laponite®) have been dewatered through different techniques: centrifugation, mechanical compression, and osmotic stress (dialysis against a polymer solution). The positional and orientational correlations of the particles have been determined through Small Angle Neutron Scattering. Uniaxial compression experiments produce concentrated dispersions (volume fraction > 0.03) in which the platelets have strong orientational and positional correlations. The orientational correlations cause the platelets to align with their normal along a common axis, which is the axis of compression. The positional correlations cause the platelets to be regularly spaced along this direction, with a spacing that matches the average volume per particle in the dispersion. The swelling law (volume fraction vs. separation) is one-dimensional, as in a layered system. Changes in the applied osmotic pressure cause the water content of the dispersion to either rise or decrease, with time scales that are controlled by interparticle friction forces and by hydrodynamic drag. At long times, the dispersions approach osmotic equilibrium, which can be defined as the common limit of swelling and deswelling processes. The variation of the equilibrium water content with the applied osmotic pressure has been determined over one decade in volume fractions ($0.03 < \phi < 0.3$) and 3 decades in pressures. This equation of state matches the predictions made from the knowledge of the forces and thermal agitation for all components in the dispersion (particles, ions and water).

Introduction

Laponite is a synthetic clay of the hectorite type, consisting of nanometric platelets [1, 2]. When water is added to a Laponite powder, the clay particles become ionized and the interstitial solution pushes the platelets away from each other, causing the grains of powder to swell with water. With appropriate mixing procedures, a clear dispersion of clay in water can be obtained. Such clay dispersions have applications in coatings, paints, cosmetics, as well as in drilling fluids, mainly because they have unusual flow properties. They have also been the subject of numerous studies, because they are well-defined materials, and yet behave in ways that are still largely controversial and unexplained.

Semi-dilute dispersions

In the range of volume fractions $0.0048 \leq \phi \leq 0.03$, Laponite dispersions have very unusual flow properties. They have a yield stress, i.e. they behave as soft solids at rest, but the application of sufficient stress causes them to flow [3-7]. The flow pattern is unusual, since it consists mainly of shear bands [4]. Moreover, these properties depend on time in a remarkable way: if a constant stress is maintained, and that stress is below the dynamic yield stress, the dispersion creeps very slowly, but it becomes more and more stiff as it ages; on the other hand, if the applied stress is above the yield stress, the dispersion starts flowing, and it becomes more and more fluid as the stress is maintained (i.e. it rejuvenates) [8-10].

A number of theories have been proposed to explain these remarkable flow behaviors [5-7, 11]. There is a class of theories that explain the resistance to flow by an aggregation process, caused by edge-face or edge-edge attractions between the particles. For dispersions that have a finite ionic strength (at least 10^{-3} mol L^{-1}), these attractions may overcome the face-face repulsions and produce a macroscopic network that opposes the flow. Other theories are based on interparticle repulsions only [8-10]. For dispersions that have an extremely low ionic strength (much below 10^{-3} mol L^{-1}), these repulsions may become so strong that they oppose any relative motions of the particles, and in this way inhibit the flow.

The aim of the present work is not to get involved in these interesting problems, but rather to explore the more concentrated dispersions.

Highly concentrated dispersions

Dispersions with a much higher volume fraction of solids occur in coatings (e.g. film formation through evaporation), and also in drilling fluids (e.g. cake formation through filtration). In both applications, it is extremely important to control the processes by which the dispersions will either release water, swell with water, or simply let water permeate through. However, such high volume fractions ($\phi \geq 0.03$) have rarely been studied so far, because highly concentrated Laponite dispersions cannot be prepared conveniently through mechanical mixing of the powder in water. They can, however, be obtained by preparing a semi-dilute dispersion that is as homogeneous as possible, and then extracting water to reach the desired volume fraction [12-20]. In this work, we have explored the range of volume fractions $0.03 < \phi < 0.4$

At these concentrations, the volume per particle is reduced so much that neighboring particles can no longer rotate independently from each other, and therefore the orientations of neighboring particles must be correlated [18]. The volume fraction threshold for orientational correlations may be predicted as follows. First, assume that the rotation volume of a particle is a sphere with a diameter equal to the platelet diameter, i.e. $2R$ = 30 nm. Then, assume that these spheres are randomly packed in the dispersion, at the volume fraction of dense random packing (0.64). Then, the volume fraction that is occupied by the platelets is related to their thickness $2H$ and diameter $2R$ by:

$$\phi^c = 0.64 \frac{\pi R^2 2H}{(4/3)\pi R^3} = 0.96 \frac{H}{R} \qquad (1)$$

Taking the accepted dimensions of the platelets ($2H$ = 1 nm, 2R = 30 nm) yields $\phi^c = 0.032$. Hence, in all dispersions of higher ϕ^c, there must be some correlations between the orientations of neighboring particles. Of course, these orientational correlations may be short range only. However, Onsager predicted that systems of anisotropic particles must have a phase transition to a phase with long-range orientational order when the particles are sufficiently anisotropic and their volume fraction is high enough [21]. The occurrence of a phase with orientational order would then have profound consequences for the mechanical properties and also for the permeability of the paste.

For clay dispersions with much larger particles (kaolinite, diameters 1-2 μm), Perdigon-Aller et al. have found that the application of uniaxial osmotic pressure causes the particles to align with their normal along the axis of compression [22]. The resulting filter cakes have a high volume fraction, high orientational order parameter and low permeability. However, this orientational order is static rather than thermodynamic, since the particles are so large that their motions are essentially blocked. Hence, the equilibrium organization of very small platelets that are able to sample a wide variety of configurations is a problem of a different nature.

To our knowledge, there are 3 experimental evidences for the existence of an orientational phase transition in Laponite dispersions. Gabriel et al. and Lemaire et al. made concentrated dispersions by slow evaporation [18, 19]. In dispersions that had been concentrated to volume fractions above $\phi = 0.02$, they observed optical textures that were characteristic of a nematic liquid. They also obtained anisotropic X-ray scattering patterns, which they used to calculate a nematic order parameter. Mourchid et al used osmotic stress to extract water from dilute Laponite dispersions [12, 13]. In dispersions that had been equilibrated for one month, they found that the rise of osmotic pressure with volume fraction was interrupted by a plateau, which they took as a sign of a 2-phase equilibrium. Remarkably, none of these authors have observed positional correlations, even though the laponite volume fractions were high enough to cause strong interactions between neighboring particles.

Questions

The experimental results available so far raise some obvious questions concerning the structures of Laponite dispersions: Do these dispersions have long-range orientational order, as in a nematic phase, or do they have only short range *orientational correlations*, as in tactoids? Do they also have *positional correlations* between the centers of the particles, and if so what is the range of these correlations: long range, as in a smectic phase, or short range as in a nematic? And in which way do these correlations derive from interparticle forces?

Such questions are usually stated with the implicit assumption that it is possible to determine the equilibrium structure, i.e. the average organization, at equilibrium, of particles, ions and water in the dispersion. However, this is not at all obvious. Even in the semi-dilute regime, the state of the dispersions has been found to evolve through some extremely slow processes [5, 7, 8, 9]. Such

observations raise serious questions about the possibility of reaching an equilibrium state in highly concentrated dispersions. These concerns lead to a large number of interesting problems, which can be grouped as follows.

Compression processes: How difficult is it to reach the highly concentrated range? What are the forces that oppose compression: are they long range or medium range forces such as ionic repulsions, or is it rather local friction between particles that are in contact? If a constant force is applied, does the dispersion reach quasi-static equilibrium in a finite time, and is this equilibrium the same with different compression techniques? Alternatively, does the dispersion evolve forever?

Expansion processes: How reversible are the extraction of water and the structural ordering that follows: if water is added to a highly concentrated dispersion, will it be absorbed and distributed within the dispersion? If so, what are the forces that cause this reswelling? And again, does the dispersion ever reach osmotic equilibrium, or does it take an infinitely long time to swell?

Equation of state: When osmotic equilibrium is reached, what is the equilibrium water content, and how does it vary with the applied osmotic pressure? Can the relation of osmotic pressure to water content be predicted from the knowledge of the forces and thermal agitation that act on all species in the dispersion (particles, ions, and water)?

Materials

We used Laponite XLG, a synthetic hectorite produced by Rockwood Additives [1]. It consists of particles that are shaped as platelets with thickness $2H$ = 1 nm, diameter $2R$ = 30 nm [1, 2], and mass per unit volume 2530 Kg/m^3 [23] (for the precise determination of H, see "Results"). The composition of this material is:

$$Si_8\left[Mg_{5.45}Li_{0.4}H_4O_{24}\right]Na_{0.7}$$

In aqueous media, the Na^+ cations are hydrated and released in the water layers surrounding each particle. They can also be exchanged by other cations; the cationic exchange capacity (CEC) is 650 mM/Kg [24] (note that for Laponite RD, Levitz et al. have found 750 mM/Kg [10]). The surface charge created by the release of these cations amounts to 0.7 e per nm^2 of surface, or 1.4 nm^2 per elementary charge. For a platelet with the dimensions given above, this yields 500

exchangeable cations on each face. These cations produce a repulsion between neighboring platelets, which is at the origin of the spontaneous dispersion of Laponite in water.

The Laponite particles were dispersed by stirring in aqueous phases that were either distilled water containing sodium chloride at a concentration of 10^{-3} mol L^{-1}, or sodium chloride at 10^{-3} mol L^{-1} and tetrasodium diphosphate at a concentration of 5.77×10^{-3} mol L^{-1}. The diphosphate anion binds to the edges of the platelets, and in this way reduces the strength of edge-face and edge-edge attractions. This has a dramatic effect on the flow properties of semi-dilute dispersions: for instance, dispersions of volume fraction ϕ =0.012 behave as soft solids (yield stress = 40 Pa) in absence of phosphates, but if phosphates are added they flow as shear-thinning fluids (no measurable yield stress) [7].

All dispersions were prepared at the same initial volume fraction ϕ =0.012, and then aged in closed vessels for 75 days. During this aging, the dispersions, initially turbid, became more transparent. In closed vessels, the pH rose from 9 to 10 over the first 25 days, and then remained stable. The concentration of Na^+ ions also remained stable at 6.5×10^{-3} mol L^{-1} (for the dispersions without phosphates) or 2×10^{-2} mol L^{-1} (with phosphates). Finally, the concentration of Mg^{++} ions decayed from 5×10^{-4} to 1×10^{-4} mol L^{-1} (without phosphates), or from 1×10^{-2} to 1×10^{-3} mol L^{-1} (with phosphates), due to the precipitation of $Mg(OH)_2$ at high pH. From these measurements, we concluded that the dissolution processes were effectively blocked by the initial rise in pH [7].

In semi-dilute dispersions made at ϕ =0.01, the background salt (NaCl and tetrasodium diphosphate) controlled the ionic strength and the ionic repulsions between neighboring particles. Indeed, the screening length that characterizes the decay of electrical potentials is κ^{-1} = 4 nm in dispersions without phosphates and κ^{-1} = 2 nm in dispersions with phosphates. On the other hand, in concentrated dispersions (ϕ = 0.1 and above), the Na^+ counterions of the Laponite particles were much more numerous than those originating from the background salt. Consider for instance two Laponite platelets that are parallel and separated by a distance of 10 nm. The interstitial solution that separates these platelets contains 1000 counterions. The average concentration of counterions in this solution is 0.25 mol L^{-1}. This is much higher than the concentration of ions originating from the added salt (6.5×10^{-3} mol L^{-1}) or from the added diphosphates (2×10^{-2} mol L^{-1}). Therefore ionic repulsions between neighboring particles can be

expected to become similar in all dispersions regardless of added salt when the particle concentration is sufficiently high ($\phi = 0.1$).

Methods

Three different methods were used in order to extract water from the semi-dilute Laponite dispersions and produce dispersions with a higher volume fraction: ultracentrifugation, mechanical compression and osmotic stress.

Ultracentrifugation

Ultracentrifugation produces a buoyancy force that tends to lift water towards the top of the tubes and push particles to the bottom (Figure 1). If the dispersions have an osmotic pressure, equilibrium is reached when this buoyancy force is balanced, at each height in the sample, by the gradient of osmotic pressure [25]. Similarly, if they have a compressive yield stress (i.e. osmotic resistance), mechanical equilibrium is reached when the applied force is balanced by the gradient of the osmotic resistance [26]. The equilibrium condition can be written for a slice of thickness ds, located at a distance s from the top of the sediment, and submitted to an acceleration $\gamma(s)$. In this slice, the lift force that pulls water towards the top of the sample is $\Delta\rho\ \gamma(s)\ \phi(s)\ ds$, where $\Delta\rho$ is the difference in mass per unit volume between the particles and water. This force is balanced by the difference in osmotic resistance $d\Pi$ between the slices located above and below:

$$d\Pi = \Delta\rho\ \gamma(s)\ \phi(s)\ ds \tag{2}$$

This equation can be integrated to give the osmotic resistance at each height:

$$\Pi(s) = \int_0^s \Delta\rho\ \gamma(s)\ \phi(s)\ ds \tag{3}$$

Accordingly, there is a gradient of osmotic resistance, with zero pressure at the top ($s = 0$) and maximum pressure at the bottom ($s = s_{max}$). At equilibrium, the osmotic resistance of the dispersion is related to its volume fraction by a constitutive equation (or an equation of state). Thus, the constitutive equation of the dispersion may be determined in a single experiment by measuring the volume fraction profile within the centrifugation tube at equilibrium, and calculating the corresponding pressure through equation (3). Experimentally, the relation of

osmotic resistance to volume fraction approaches the true equation of state as the dispersion approaches equilibrium during centrifugation.

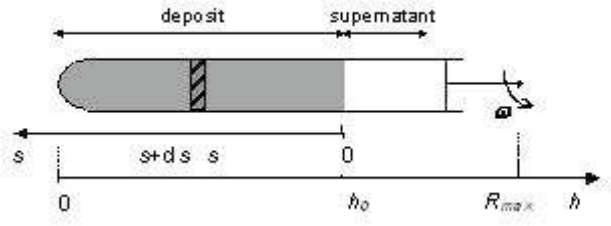

Figure 1. Geometry of the centrifugation experiment. The slice located between heights *s* and *s+ds* is submitted to a centrifugal force, which tends to push the particles towards the bottom of the tube and water to the top. At equilibrium, this is equilibrated by the gradient of osmotic pressure exerted by the slices located immediately above and below this slice.

A Kontron Instruments Centrikon T-1080 centrifuge with swinging bucket rotor was used. With this instrument, the acceleration γ varied with the distance *s* from the top of the sediment (given in mm) and with the rotation speed ω (given in rpm) according to:

$$\gamma = 1.12\left(R_{\max} - h_0 + s\right)\left(\frac{\omega}{10^3}\right)^2 \qquad (4)$$

where R_{max} is the distance between the center of the rotor and the bottom of the centrifuge tube in the horizontal position, and h_0 is the height of the sediment at the end of the centrifuge cycle. With a rotation speed ω =12000 rpm, the acceleration γ was 12150 g_a (with g_a acceleration of gravity) at the top of the tube and 26000 g_a at the bottom; with ω =23000 rpm, it was 44615 g_a at the top of the tube and 95510 g_a at the bottom. In samples obtained with this swinging bucket rotor centrifuge, the deposits were collected by removing the supernatant and then cutting the tubes into slices 1-2 mm thick [25, 26]. The volume fractions of these slices were then measured by thermogravimetry (drying at 120 °C). The experimental volume fraction profile was then fitted by a polynomial expression:

$$\phi(s) = \sum_{i=0}^{i=n} a_i \; s^i \tag{5}$$

This profile was then inserted into equation (3), giving the following expression for the osmotic resistance:

$$\Pi(s) = \Delta\rho\, \omega^2 \left[(R_{\max} - h_0)\, a_0\, s + \sum_{i=1}^{i=n} \frac{(R_{\max} - h_0)\, a_i + a_{i-1}}{i+1}\, s^{i+1} + \frac{a_n}{n+2}\, s^{n+2} \right] \tag{6}$$

Concentrated dispersions were produced through a protocol that consisted of several centrifugation cycles. In each cycle, the supernatant was removed and additional dispersion was introduced into the centrifugation tube. Each cycle lasted at least 10 hours for centrifugation at 23000 rpm and 2 days at 12000 rpm; in some experiments, centrifugation was continued for 15 days. These unusually long cycles were chosen in order to give as much time as possible to equilibration processes that determine the relation of osmotic resistance to volume fraction.

Mechanical compression

In mechanical compression, a compressive stress is applied to the boundaries of the sample, while water is allowed to permeate out through filtration membranes [27]. The compressive stress is transmitted through interparticle forces; since no other force is applied to the particles, the stress is uniform throughout the sample. At equilibrium, the volume fraction is determined by the value of the compressive stress through a constitutive equation. Therefore the constitutive equation may be determined through a set of compression experiments in which the dispersions are equilibrated at different pressures.

A bilateral filtration cell was used for mechanical compression experiments. The cell body was a stainless steel tube (inner diameter 72 mm). It was closed with 2 pistons made of sintered stainless steel (pore diameter 100 μm) covered by ultrafiltration membranes (average pore diameter 0.05 μm). A constant uniaxial force was applied to one piston, and the resulting displacement was measured with an accuracy of 0.01 mm. The compressive force was maintained until there was no measurable change in position, which took about 7 days. At the end of

compression, the sample was recovered and its volume fraction was measured through thermogravimetry.

Osmotic stress

In osmotic stress, the driving force (for the extraction of water) is the difference in chemical potential between water in a "stressing solution" and water in the dispersion [28]. At equilibrium, the chemical potentials of water in the solution and in the dispersion are equal; therefore the osmotic resistance of the dispersion matches the osmotic pressure of the stressing solution. At this point the dispersion is recovered and its volume fraction is measured. If the osmotic pressure of the stressing solution is known, the measurement yields one point of the constitutive equation of the dispersion. In practice, a large number of osmotic stress experiments are performed in parallel, yielding a corresponding set of data points for the constitutive equation.

For osmotic stress experiments, semi-dilute dispersions of Laponite were placed in Visking dialysis bags that had a pore size corresponding to a 12K molecular weight cutoff (Spectrapor, Spectrum, USA). These bags were immersed into Dextran solutions for a succession of water extraction cycles. At the end of each cycle, the deswelled bag was refilled with additional dispersion and the Dextran solution was replaced. The final cycle lasted 3 weeks. At this point, the dispersion was recovered and its volume fraction was measured through thermogravimetry.

Small angle neutron scattering (SANS)

In neutron scattering, incident neutrons are scattered by the nuclei located in the irradiated volume; a nuclear scattering length characterizes the strength of the interaction between a neutron and each nucleus. In small angle scattering, the distances between neighboring atoms are not resolved. Instead, the interferences of scattered rays depend on the distances between small volume elements, each containing large numbers of nuclei; the contribution of each volume element is weighted by its density of scattering length $\rho(\mathbf{r})$ [29]. For Laponite dispersions, the density of scattering length takes only two values, one in water and one in the particles. A homogeneous sample, containing water only, would give no scattering in directions outside the beam, hence the scattering is due to fluctuations in the density of scattering length, caused by the distribution of particles in water.

The phase differences that control the interferences of scattered rays are determined by the scalar product **Q.r**, where **r** is the vector joining 2 nuclei, and **Q** is the scattering vector. The magnitude of the scattering vector depends on the neutron wavelength λ and scattering angle θ according to:

$$Q = \frac{4\pi}{\lambda} \sin\frac{\theta}{2} \qquad (7)$$

In the present work, we used Q values ranging from 0.1 to 3 nm^{-1}, corresponding to real space distances between 60 and 2 nm respectively.

The measured interference pattern is a Fourier Transform of the pair correlation function P(r) of the spatial variation of Δρ:

$$I(\mathbf{Q}) / I_{incident} = \int P(r) \exp (i\, \mathbf{Q.r})\, d\mathbf{r} \qquad (8)$$

$$P(r) = \int \Delta\rho(\mathbf{r'})\, \Delta\rho(\mathbf{r}+\mathbf{r'})\, d\mathbf{r'} \qquad (9)$$

If the relative positions of the particles are strongly correlated, then P(r) is an oscillating function, and I(**Q**) has a set of peaks located at **Q.d** = 2nπ, where **d** is lattice vector of ρ(**r**). These peaks are infinitely sharp in the case of long-range order, and broader in the case of short-range order. For instance, a lamellar structure produces a diffraction pattern that consists of sharp spots that are regularly spaced on a line that is oriented along the direction of repetition; a nematic phase gives a pattern that consists of two crescents located in the direction of the nearest neighbors [30, 31].

For dispersions that were submitted to uniaxial stress (e.g. centrifugation), slices of the sample were cut with a specific orientation with respect to the axis of compression. In this way, the interference patterns measured correlations in the relative positions of particles, in directions that were either along the axis of compression or away from this axis.

Longitudinal slices were cut along the length of the centrifugation tube, so that the axis of compression was within the plane of the slice (Figure 2a). These slices were placed in the neutron beam so that their axis of compression was perpendicular to the beam. In this case, the detector selected some scattering vectors that were parallel to the axis of compression, and some that were not. These experiments made it possible to measure distances in the direction of compression.

Transverse slices were cut across the centrifugation tube, so that the axis of compression was perpendicular to the plane of the slice (Figure 2b). These slices were placed in the neutron beam

so that their axis of compression was along the beam. In this case, the detector selected scattering vectors that were exclusively perpendicular to this axis. These experiments measured distances in directions that were perpendicular to the axis of compression.

Neutron scattering patterns were obtained on the instrument D11 at ILL, with a sample-detector distances of 1.09 m, 2m and 3,5 m and a collimation distance of 5 m, using neutrons of wavelength 6 Å.

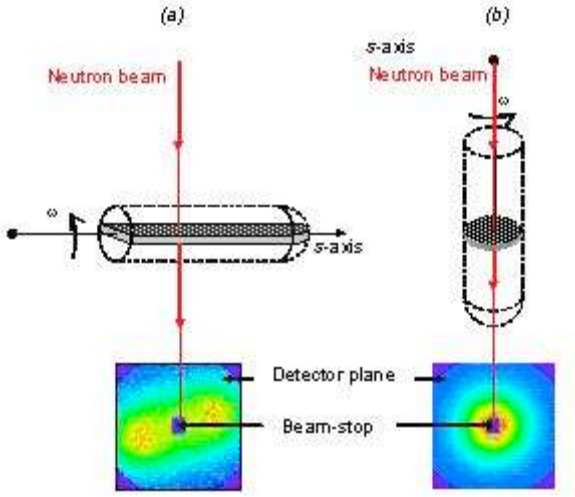

Figure 2. Recovery of slices cut from the sediment. (a) Slices that are cut along the axis of compression. (b) Slices that are perpendicular to the axis of compression.

Results

In this section, we first report the neutron scattering patterns of the compressed dispersions, because these patterns immediately show how the platelets organize during the compression. Then we present measurements of the volume fractions that are reached in each compression experiment, and their relation to the applied osmotic pressure. The relation of pressure to volume fraction is the compression law of the dispersion in the given conditions; if the system were at equilibrium, this would be its equation of state. The dispersions, however, have been found to evolve very slowly towards an equilibrium that is never reached. For this reason, the location of the true equilibrium state will be determined through the comparison of osmotic processes that start from higher and from lower water contents, and converge towards the equilibrium swelling.

Structures of compressed dispersions

When the dispersions were centrifuged at high accelerations (95500 g_a at the bottom of the tube) for a long time (15 days), their neutron scattering patterns revealed a remarkable structural organization. This was obvious in slices of the sediment that were cut and oriented in such a way that the plane of scattering vectors contained the axis of compression (Figure 2a). In all sections where the volume fraction of Laponite was at least $\phi \geq 0.09$, the interference pattern consisted of 2 bright spots located on either side of the beam, in the direction of the axis of compression (Figure 3).

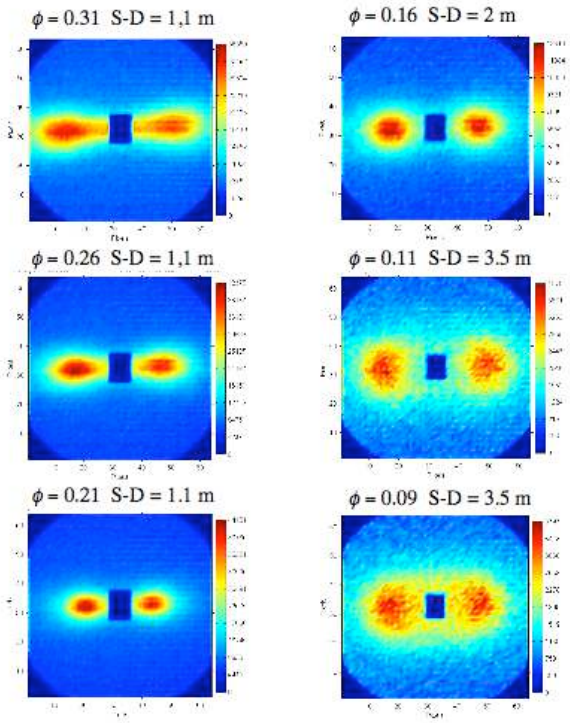

Figure 3. Interference patterns obtained from a slice that was cut along the axis of compression, and oriented normal to the neutron beam, so that the plane of scattering vectors (i.e. the plane of the Figure) contained the axis of compression (approximately horizontal in the Figure). Each pattern was obtained by aiming the beam at a particular height *s* within the slice (see Figure 1). The corresponding volume fraction ϕ was read from the height vs. volume fraction profile of the sediment, which was centrifuged for 15 days at a maximum acceleration of 95500 g_a. The patterns show two bright spots that move away from the beam (taking into account the sample-detector distances indicated in the labels) as the volume fraction is increased.

Such spots must originate from Bragg diffraction by planes that are oriented normal to the axis of compression. However, the spots are rather broad, and they are not accompanied by higher diffraction orders. Hence they result from diffraction by a pseudo-periodic variation of the density of scattering length in the direction of compression. In dispersions where the volume fraction of platelets is $\phi = 0.1$, the period is 10 nm, which is about 10 times the platelet thickness. Thus, the locations of the spots match the diffraction pattern of a system of platelets that are oriented parallel to each other, with their normal along the axis of compression, and that are regularly spaced along this direction. The width of the spots indicates that there is short range order only (correlation length 30 nm) rather than long range order; however, there is no evidence of significant disorientations in the structure, that would cause the diffraction spots to take the shape of "crescents".

Slices that were cut and oriented in the other direction (Figure 2b), so that the plane of scattering vectors was perpendicular to the axis of compression, did not show any such features (Figure 4). These interference patterns show a monotonic decay of the intensity in all directions that are normal to the axis of compression. Therefore, there are no periodic correlations in these directions. The decay rate of the intensity matches approximately the particle diameter; therefore, any correlations in these directions are lost at larger distances. Identical observations were made on Laponite dispersions where phosphates had been added.

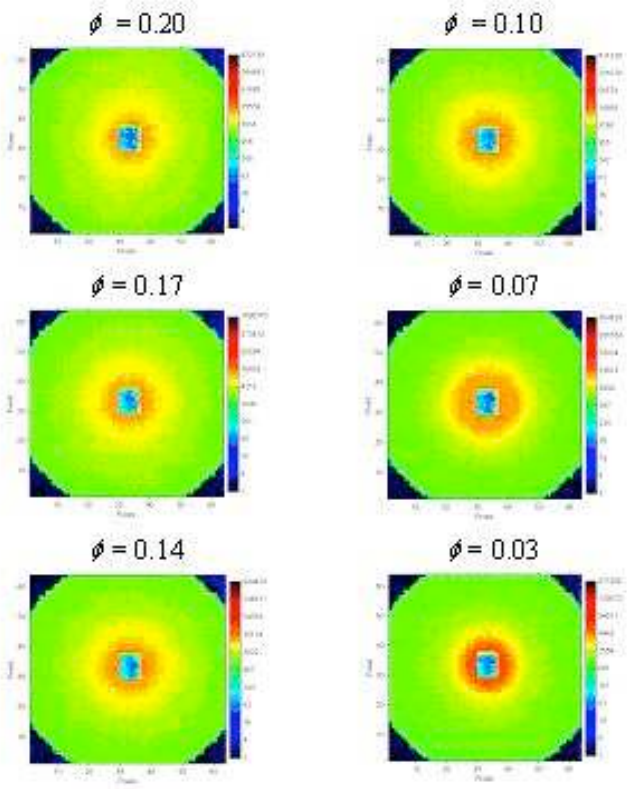

Figure 4. Interference patterns obtained from a slice that was cut perpendicular to the axis of compression, and oriented normal to the neutron beam, so that the plane of scattering vectors was normal to the axis of compression (i.e. the plane of the Figure is normal to the axis of compression). The slice was cut from a sediment that was centrifuged for 15 days at a maximum acceleration of 95500 g_a.

The structures that produce such scattering patterns can be described in two ways [30, 31]. One description is based on a nematic structure, with long-range orientational order and short-range positional order. The platelets are parallel to each other, with their normal aligned along the common axis. In the direction of this axis, they have short-range order, i.e. face-to-face separations that fluctuate around an average distance. In directions perpendicular to this axis, they have no order at all, i.e. they are not organized in columns, as would have been the case for "stacks of plates". The other description is based on a lamellar structure, with short-range order for the repetition of the layers, but no order within each layer. From a structural point of view,

both descriptions are completely equivalent; their main feature is the strong positional correlations that were absent in interference patterns of dispersions made at lower volume fractions.

As the volume fraction of Laponite was increased, the spots moved away from the beam, indicating that the repeat distance of particles in the dispersion became shorter. Remarkably, this distance was found to vary linearly with the inverse volume fraction $1/\phi$, in agreement with the swelling law expected for one-dimensional swelling of a stack of layers with thickness $2H$ and separation $2h$:

$$d = 2(h + H) = \frac{2H}{\phi} \qquad (10)$$

The slope of the variation of d as a function of $1/\phi$ yields the average thickness of the platelets, which is found to be $2H$ = 1.35 nm. The same variation was found for dispersions with added phosphates, which was expected since they are made of the same platelets (Figure 5).

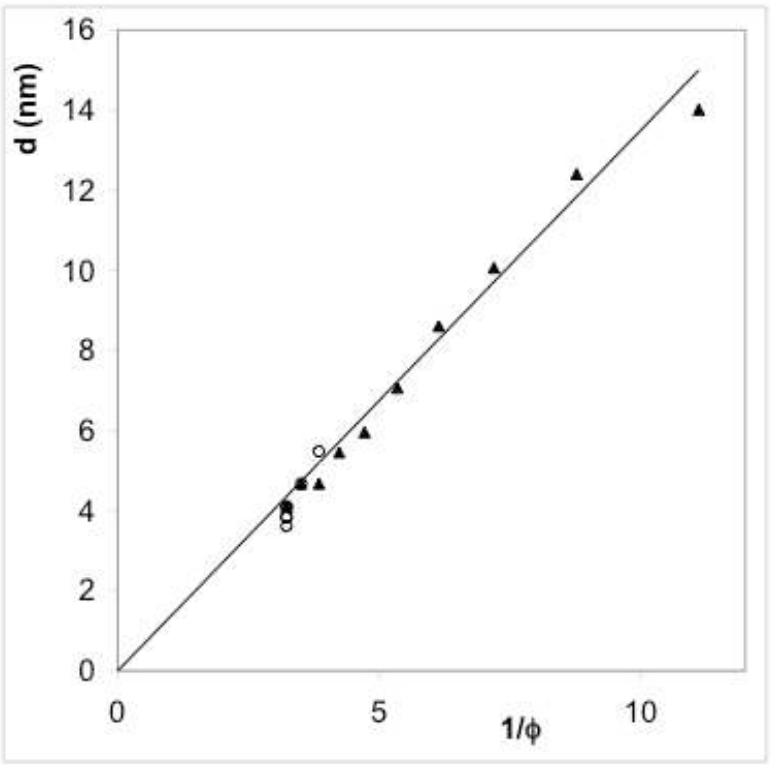

Figure 5. Variation of the repeat distance d of the layers with the inverse of the volume fraction ϕ. Symbols: (▲) dispersions without phosphates; (O) with phosphates. A linear variation is

expected for systems that swell in one dimension only. In this case, the slope of this variation yields the thickness *H* of the dry layers. The straight line corresponds to H = 1.35 nm.

At lower volume fractions, the spots merged with the beam, but the diffraction patterns remained anisotropic (similar observations were made previously through X-ray scattering [19]). Therefore the organization of Laponite dispersions evolves in two stages during compression: in a first stage ($0.02 < \phi < 0.05$), the platelets have strong orientational correlations but only weak positional correlations, and the swelling law must be a 3-d swelling law, as in a nematic; in a second stage, the positional correlations also become quite strong, and the swelling law becomes the one-dimensional swelling law of a layered system.

Compression processes

The Laponite dispersions were compressed through centrifugation at 95500 g_a (at the bottom of the tube) over periods of 1-15 days. According to the sediment heights, sedimentation was practically complete within 1 day. Still, the volume fraction profiles within the sediment evolved over longer times. The volume fractions profiles were measured in sediments that were centrifuged either 7 days or 15 days, and the corresponding osmotic resistances were calculated as explained in "Methods". Figure 6 presents the variation of osmotic resistance with volume fraction for each sediment. All experiments show a steep increase of the osmotic resistance Π with volume fraction ϕ. However, for a given pressure, the volume fraction that the dispersion reaches at longer times (15 days) is slightly higher than that obtained at shorter times (7 days); the ratio is highest at the lowest pressures (4×10^5 Pa), and it reaches unity at the highest pressures (8×10^6 Pa). These observations show the relevance of a question raised in the introduction: how do we know that the dispersion has reached quasi-static equilibrium?

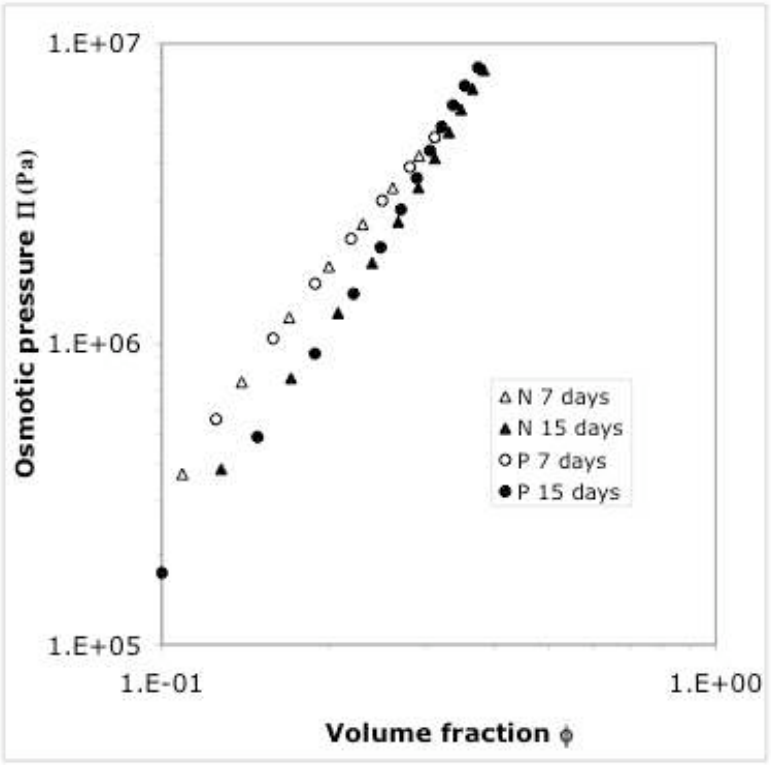

Figure 6. Effect of compression time on the osmotic resistance of Laponite dispersions. Horizontal scale: volume fractions of slices recovered from each centrifugation experiment. Vertical scale: osmotic pressures calculated from the location of the slice in the centrifugation tube, the volume fraction profile, and the acceleration. Open symbols: slices recovered after 7 days of centrifugation. Filled symbols: slices recovered after 15 days of centrifugation. Δ, ▲: No phosphates (N); O, ●: with phosphates (P).

A similar problem was encountered when dispersions were centrifuged at different accelerations. Dispersions that were centrifuged at a lower acceleration (26000 g_a at the bottom of the tube), and therefore submitted to a lower osmotic pressure gradient, gave volume fractions that were slightly lower (Figure 7). This small difference indicates that the compression processes are slower at the lower acceleration, presumably because the sediment is thicker, and the times required for the diffusion of water are slower. In those conditions, the measured volume fractions are below the true equilibrium volume fractions at the set osmotic pressure.

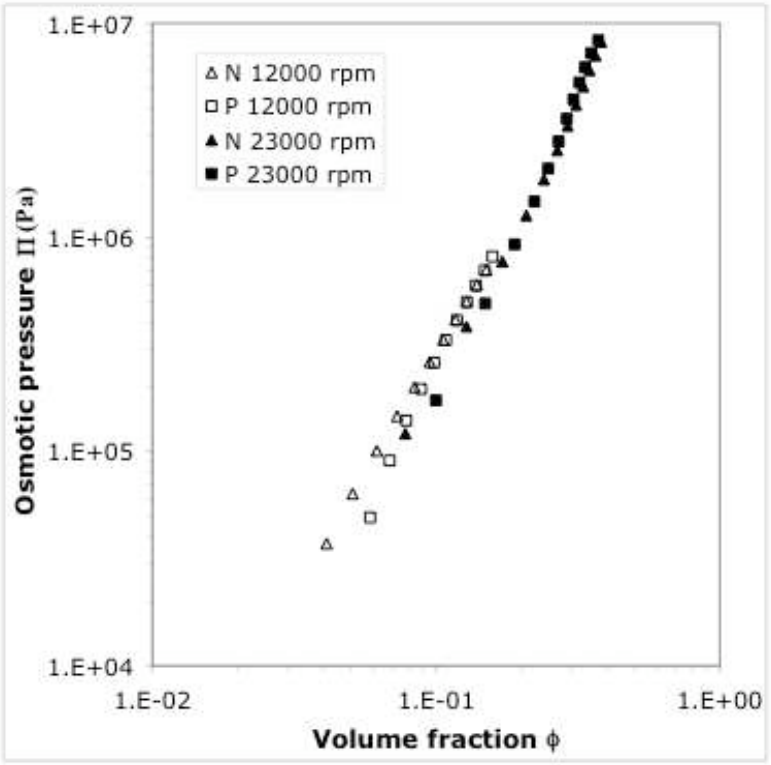

Figure 7. Effect of the set acceleration on the osmotic resistance measured through centrifugation. Open symbols: centrifugation at 12000 rpm, maximum acceleration = 26000 g_a; filled symbols: 23000 rpm, maximum acceleration = 95500 g_a; Δ, ▲: no added phosphates (N); O, ●: with added phosphates (P).

Similar experiments were conducted with Laponite dispersions that contained phosphates. With these fluid dispersions, the kinetics of sedimentation was different [7], but the final profiles of volume fraction and osmotic pressure were exactly the same as in the dispersions that contained no phosphates. As shown in Figures 6 and 7, the curves for both dispersions are indeed identical, excepted for the lowest pressures, where the dispersions that contained phosphates reached slightly higher volume fractions.

At this point it is useful to compare the values of the osmotic resistance that have been obtained through different compression methods. The same Laponite dispersions have been compressed through the application of a mechanical force or through osmotic stress [27]; similar types of Laponite have also been submitted to mechanical compression at very high pressures [14, 15], or

to osmotic stress at lower pressures [12, 13]. All these data are compiled in Figure 8. Here again the experiments performed over longer periods of time reach higher volume fractions for a given applied volume fraction. These comparisons demonstrate that there is a very slow creep process by which dispersions submitted to a constant osmotic pressure evolve towards higher volume fractions. It is therefore important to find out whether there exists, at each applied force, a volume fraction at which thermodynamic equilibrium is reached. For this purpose, we have performed experiments in the other direction, i.e. through reswelling instead of deswelling.

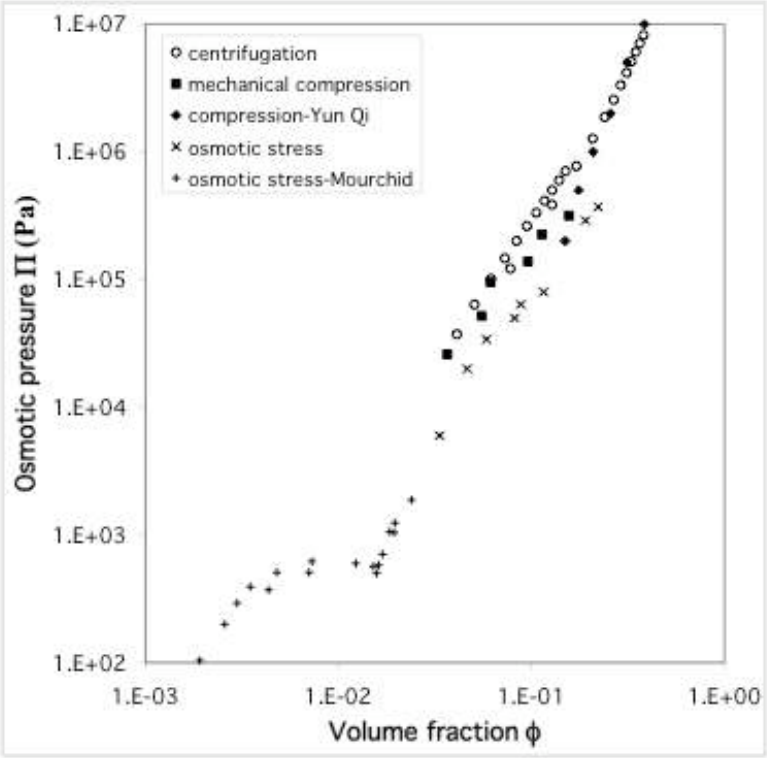

Figure 8. Osmotic resistances measured through different compression techniques. Symbols: o, centrifugation (this work); ■, mechanical compression (this work); ◆, mechanical compression [14, 15]; x, osmotic stress (this work); +, osmotic stress [12, 13]. Note that the data extend over 3 decades in volume fractions and 5 decades in osmotic pressures.

Expansion processes

Two Laponite dispersions were compressed for 15 days at the highest acceleration (95500 g_a at the bottom of the tube), and then kept in the centrifuge at a lower acceleration (26000 g_a,) for another 15 days. Visual observation of the tubes indicated that the sediment did reswell during

the second period. This reswelling indicated that the dispersion had a true osmotic pressure, and not only a mechanical resistance to compression.

At the end of this second period, the sediments were recovered, the volume fraction profiles were measured, and the osmotic pressures corresponding to the final acceleration at each location in the tube were calculated. The relation of pressure to volume fraction obtained at the end of this combined cycle (deswelling at 95500 g_a followed by reswelling at 26000 g_a) was compared with that obtained through direct deswelling at the same final acceleration (Figure 9). The volume fractions obtained at the end of the combined cycle were systematically higher than those that were reached through direct deswelling at 26000 g_a. This difference can result from incomplete reswelling in the combined cycle, or incomplete deswelling in the direct experiment, or from a mixture of both. In any case, the equilibrium volume fraction must be lower than that obtained at the end of reswelling, and higher than that reached through direct deswelling, so that it must lie between both curves.

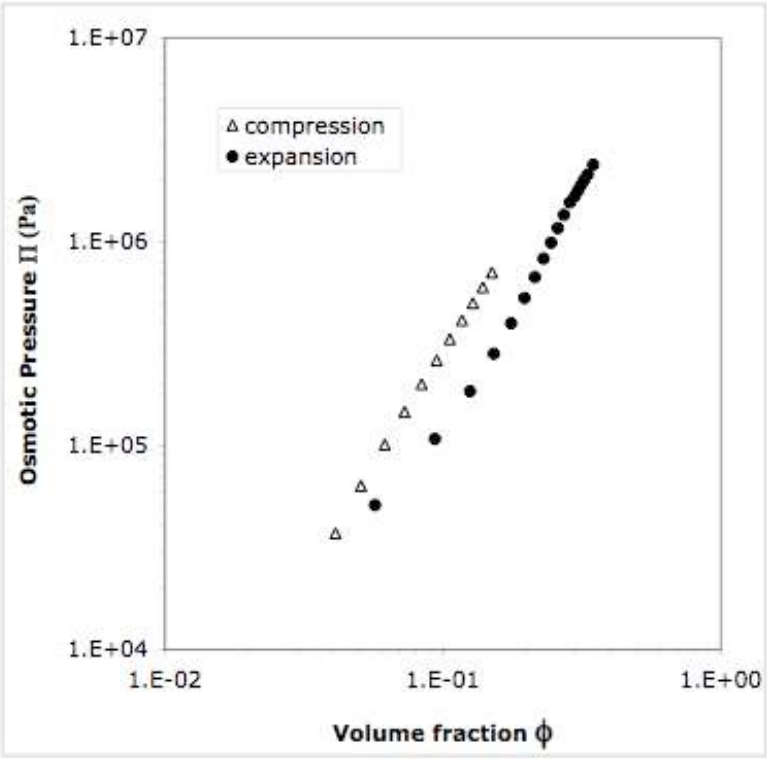

Figure 9. Osmotic pressures measured through a swelling experiment, and comparison with a compression experiment, both using centrifugation, for a dispersion without phosphates. Symbols: Δ, data from a dispersion that was compressed through centrifugation at 26000 g_a for

15 days. ●, data from a dispersion that was first compressed through centrifugation at 95500 g_a for 15 days, and then allowed to reswell during centrifugation at 26000 g_a for 15 days.

At this point it is useful to compare the volume fractions obtained through this reswelling experiment with those that were reached through osmotic stress in 30 days. Figure 10 presents this comparison in the case of dispersions that contained no phosphates. Reswelling after centrifugation and osmotic stress yield nearly the same relation of pressure to volume fraction. Again, the equilibrium volume fraction must be lower than that obtained at the end of reswelling, and higher than that reached through direct deswelling, so that it must lie between both curves. Since both experiments give the same relation, within experimental uncertainties, they both provide a determination of the equilibrium volume fraction in this range of pressures, i.e. pressures ranging from 2×10^4 to 2×10^6 Pa, and volume fractions between 0.05 and 0.25.

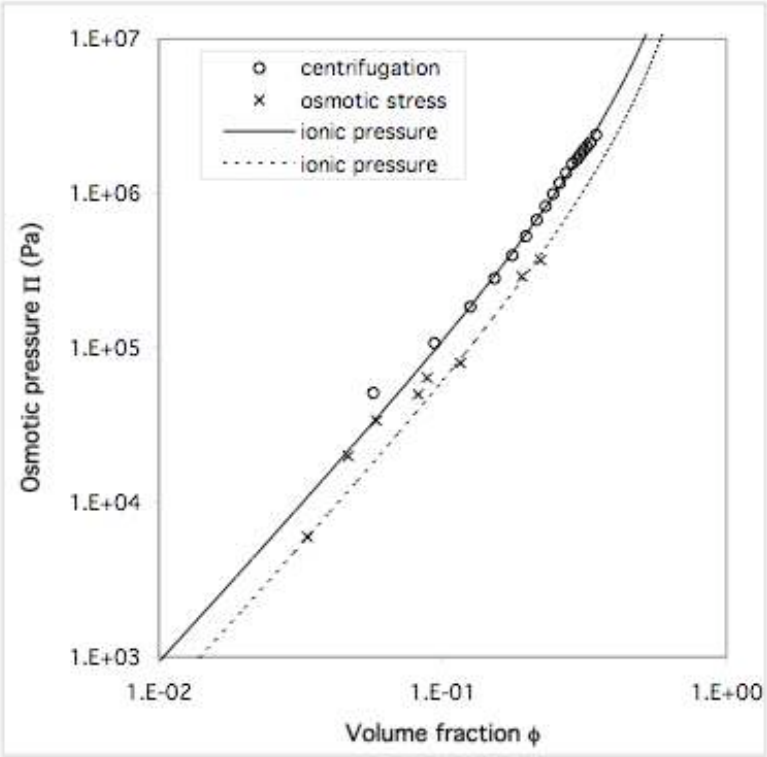

Figure 10. Osmotic pressures measured through a swelling experiment, and comparison with the osmotic stress experiment. Symbols: (o), data from a dispersion that was first compressed through centrifugation at 95500 g_a, and then allowed to reswell during centrifugation at 26000 g_a; (x), data from a set of dispersions that were submitted to osmotic stress for 3 weeks. Full line:

theoretical pressures due to the resistance to compression of the layers of counterions, calculated for a platelet thickness $2H$ = 1 nm. Dashed line: same with $2H$ = 1.35 nm (see the text).

At lower pressures or volume fractions, the approach to equilibrium was found to become exceedingly slow. This was observed when the centrifugation tubes (containing the sediment and surpernatant) were left at rest, and the sediment height was recorded as a function of time. Figure 11 presents the variation of sediment height as a function of time, for both types of dispersions (with or without phosphates). In all cases, there is a first stage of swelling where the increment in sediment height grows as the square root of time. Then, as the sediment crosses from the concentrated to the semi-dilute range of volume fractions ($\phi \approx 0.03$), the rate of evolution slows down considerably. For dispersions with phosphates, it is about 3 times slower, and for dispersions without phosphates, at least 10 times slower. This difference in swelling laws bears a striking resemblance to the difference in rheological behavior of the semi-dilute dispersions, since the dispersions with phosphates are fluids, whereas those without phosphates are soft solids.

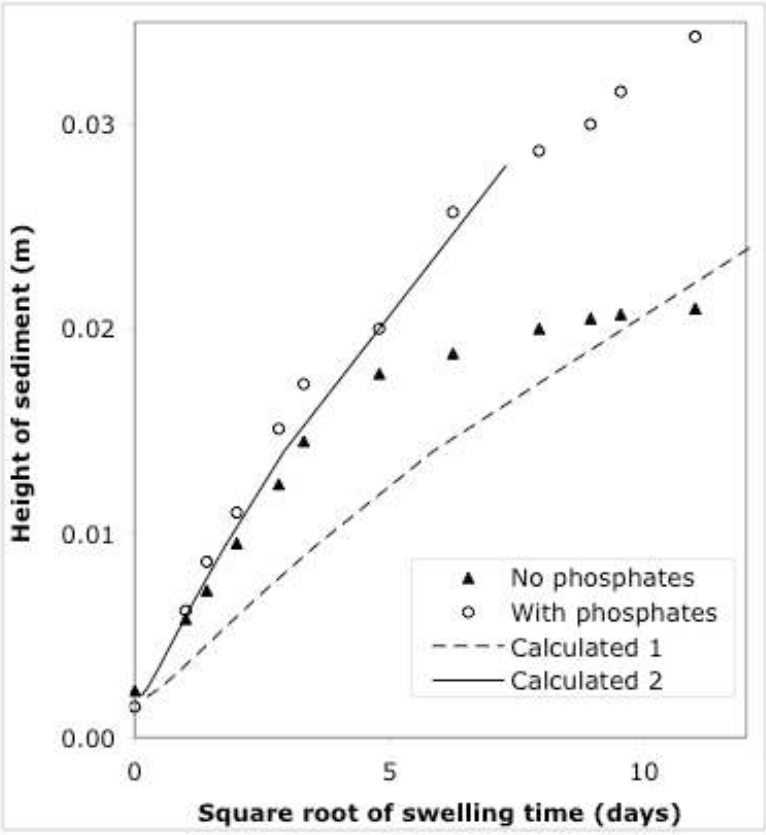

Figure 11. Kinetics of expansion for sediments that were centrifuged at 26000 g_a and then left in equilibrium with the supernatant after centrifugation. (▲) Dispersions without added phosphates; (O) dispersions with added phosphates; Lines: calculated swelling rates for simple permeation processes (see the text)

Summary of results

The central result of this work is the observation of spontaneous swelling for highly concentrated Laponite dispersions. This swelling implies that the concentrated dispersions have a true osmotic pressure. Dispersions that are submitted to an external osmotic pressure must therefore evolve towards a state where their internal osmotic pressure matches the applied pressure. This state is the osmotic equilibrium state of the dispersion.

At equilibrium, the relation of volume fraction to osmotic pressure is the equation of state of the dispersion. An approximate determination of this equation has been obtained by comparing the volume fractions of dispersions that evolved from higher volume fractions (expansion) and from lower volume fractions (compression) at the same applied pressure.

The structures of Laponite dispersions in this equilibrium state have strong orientational and positional correlations. The orientational correlations cause the platelets to align with their normal along a common axis, which is the axis of compression. The positional correlations cause the platelets to be regularly spaced along this direction, with a spacing that matches the average volume per particle in the dispersion. There are no other periodic or pseudo-periodic correlations in the structure. The swelling law (volume fraction vs. separation) is one-dimensional, as in a layered system.

The approach to this osmotic equilibrium state can take very long times, especially so at low pressures and volume fractions. At the higher pressures ($\Pi > 4 \times 10^6$ Pa) and volume fractions ($\phi > 0.3$), a quasi-static state was reached in compression or in expansion experiments after 15 days (however, the volume fractions that were reached through compression remained slightly lower than those reached through expansion). At the lower pressures (1×10^5 Pa) and volume fractions (0.1), dispersions with added phosphates were still evolving after 1000 days and dispersions without phosphates remained stuck in a state that was not their osmotic equilibrium state.

Discussion

The aim of this section is to rationalize the experimental results presented above. There are two sets of results that need to be rationalized. On the one hand, there are results that were obtained at the end of very long compression and expansion cycles. These results provide an approximate determination of the equilibrium state of concentrated Laponite dispersions: indeed, this state must be located between the states that were reached through compression and through expansion at the same pressure. In this respect, we need to rationalize the nature of this equilibrium state, i.e. figure out what is the equilibrium structure of dispersions, what are the interparticle forces in this equilibrium state, and how these forces determine the structure. On the other hand, there are kinetic results that were obtained during compression or expansion experiments: these results show how the dispersions evolve towards the equilibrium state. We would like to understand what are the forces that drive this approach to equilibrium, and what are the forces that oppose it. Moreover, we would also like to know whether these compression or expansion processes can lead to a state that is "close enough" to equilibrium in a finite time, or whether these processes can take an infinitely long time.

Osmotic equilibrium state

The equilibrium structure of concentrated dispersions has been described on the basis of the SANS interference patterns. In this structure, the particles have strong orientational correlations (the platelets tend to align their normal along a common axis), and also strong positional correlations (the platelets tend to be regularly spaced along this direction). This structure differs from those of the less concentrated dispersions, in which platelets form random aggregates when the ionic strength exceeds 10^{-3} M [7]. Therefore the compression produces a structural transition in which the aggregated particles reorganize into a lamellar structure. This reorganization must result from a shift in the relative strengths of interparticle forces.

The forces are of two types [32]:

(a) Interactions between all electrical charges, including surface charges, edge charges, and all ions in the interstitial solution.

(b) Pressures caused by the thermal agitation of the ions.

In the case of Laponite, the effects of (a) can be quite complex, because of the uneven charge distribution on the particles (positive charges on the edges, negative ones on the faces). At low volume fractions and moderate ionic strengths, these forces lead to aggregation (network formation) through edge-face and edge-edge attractions [7]. The effects of (b) are rather simple, since these pressures tend to prevent the overlap of the dense ionic layers that are located next to the surfaces. This distinction between two types of forces makes it easier to understand the structural transition that takes place at high volume fractions: when the extraction of water pushes the faces of the platelets closer to each other, the cost of overlap of ionic layers becomes prohibitive, so that (b) wins over (a). At this point the particles flip into a parallel configuration, lose their edge-face contact and take regular spacings.

The relation between forces and structure also becomes simple in this situation. Indeed, the swelling pressure caused by the layers of counterions can be calculated through the Poisson-Boltzmann theory for the case where the platelets are parallel and the counterions are monovalent [32]. The resulting pressure depends on the distance $2h$ between platelets, on the surface charge density σe of the platelets (or the concentration of counterions, $2\sigma/2h$), and on the concentration of added salt (or the screening length κ^{-1}). The expression for the pressure is particularly simple in three limiting ranges of distances:

Very short distances: $h < l_G$, where l_G is the Gouy-Chapman length defined as:

$$l_G = \frac{2\,kT\,\varepsilon_0\,\varepsilon_r}{\sigma\,e^2} \tag{11}$$

In this case the concentration of counterions is uniform within the interstitial solution that separates the particles, and it is very high. Any salt that was added to the dispersion is excluded by the Donnan effect, and remains in the supernatant. The osmotic pressure of the interstitial solution is the pressure of a uniform gas of counterions, and it decays as the inverse of the separation:

$$\Pi = kT\frac{\sigma}{h} \tag{12}$$

Intermediate distances: $l_G < h < \kappa^{-1}$. In this case, passive salt is still excluded, but the counterions are not uniformly distributed within the interstitial solution. Instead, they accumulate near the

charged surfaces, giving a pressure that is independent of the surface charge density and decays as the inverse square of separation:

$$\Pi = \frac{\pi}{2}\frac{kT}{L_B}\left(\frac{1}{2h}\right)^2 \tag{13}$$

where L_B is the Bjerrum length defined as:

$$L_B = \frac{e^2}{4\pi\,\varepsilon_0\,\varepsilon_r\,kT} \tag{14}$$

Large distances: $\kappa^{-1} << h$. In this case, the added salt floods the interstitial solution and screens the surface charges. For high surface charge densities, the surface potential takes a limiting value which is ψ_{eff} = 100 mV. Because of this screening, the osmotic pressure of the interstitial solution decays exponentially with distance:

$$\Pi = 2\,\varepsilon_0\,\varepsilon_r\,\kappa^2\,\psi_{eff}^2\,\exp(-2\kappa h) \tag{15}$$

For concentrated Laponite dispersions ($0.1 < \phi < 0.4$), the interparticle separations are in the intermediate range defined above. Indeed, for lamellar structures, the half separation h is related to volume fraction ϕ through equation (10). This yields half separations that are in the range 1 nm $< h <$ 6 nm. These separations are always longer than the Gouy Chapman length, which for Laponite surfaces (σ = 0.7 charge /nm^2) is l_G = 0.32 nm. Consequently, the separations are never in the range of "very short distances".

On the other hand, at lower volume fractions, the half separation h may be comparable to the screening length κ^{-1}, which is either 4 nm or 2 nm for dispersions without or with phosphates. Thus, upon decreasing the volume fraction, there may be a crossover from "intermediate" (salt is excluded) to "large" distances (salt floods the interstitial solution). A practical way of locating this crossover is to compare the pressures measured at these different ionic strengths: as long as these pressures are identical, it can safely be assumed that the added salt has remained in the supernatant. Figures 6 and 7 show that the pressures measured for dispersions with and without added phosphates are identical, within experimental errors, at all volume fractions in the range $0.1 < \phi < 0.4$. Therefore, added salt has not been able to flood the interstitial solution, presumably

because of the very high value of the surface potential of Laponite. In these conditions the osmotic pressure is expected to follow equation (13), given above for intermediate distances.

The comparison of experimental pressures with the theoretical compression law is presented in Figure 10. The expectation was that the true equilibrium osmotic pressure should lie in between the data obtained though deswelling and through reswelling, and closest to the data from experiments with the longest time scales. The theoretical pressures were calculated through equation (13), which contains no adjustable parameters; however, the conversion of distances into volume fractions through equation (10) involves one experimental parameter which is the layer thickness $2H$. If this thickness is taken at the value given by the manufacturer ($2H$ = 1 nm), then the theoretical curve lies right on top of the reswelling data. If it is taken at the value determined from the diffraction patterns of concentrated dispersions ($2H$ = 1.35 nm), then the theoretical curves is on top of the osmotic stress data. Since both sets of experimental data are quite close to each other, and the theoretical equation of state contains no adjustable parameters, the agreement can be considered as excellent.

Another theoretical calculation was performed through a Monte Carlo simulation of the distribution of counterions in the interstitial solution that separates two parallel platelets [33]. This approach is more accurate than the Poisson-Boltzmann theory, since it takes into account all configurations of the counterions near the particle surfaces, rather than a mean-field approximation to these configurations. The results of this simulation are quite close to equation (13) at intermediate distances, and to equation (12) at very short distances. This agreement was also expected, since the Laponite dispersions do not contain divalent counterions that would take configurations that depart significantly from the mean field distributions.

Therefore the osmotic pressures that were measured through experiments with slow time scales (either osmotic stress or reswelling during centrifugation) are quite close to the equilibrium pressures that result from the thermal agitation of counterions that are located in the vicinity of the faces of the platelets.

Approach to osmotic equilibrium

Compression experiments have indicated that, for concentrated dispersions, the approach to this osmotic equilibrium state can be quite slow (2-4 weeks). Expansion experiments have also

demonstrated that the time scales can become extremely slow (months) or practically infinite at lower volume fractions (Figure 11). These long time scales indicate that the swelling is opposed by internal friction forces. There are two types of forces that can oppose the relative motions of particles and solvent: (1) hydrodynamic drag forces that oppose the permeation of water through the network of particles, and (2) interparticle forces that tend to keep the particles locked into one configuration.

There is strong evidence that, in the first stage of swelling (where the average volume fraction of the sediment is still high), the swelling rate is limited by the rate of permeation. Indeed, the permeability of ordered Laponite sediments is extremely low [27]. At a volume fraction $\phi = 0.07$, it is $k_p = 2.5 \times 10^{-18}$ m^2, and at $\phi = 0.13$ it is $k_p = 6 \times 10^{-19}$ m^2. As a comparison, clay filtercakes made of larger kaolinite particles have permeabilities $k_p = 2 \times 10^{-16}$ m^2 if the particles are aggregated, and $k_p = 3\times 1\,0^{-17}$ m^{2}if they are well dispersed [22]. Thus, the permeabilities of Laponite cakes are 100 times smaller than those of cakes made of regular clay particles. The permeabilities of Laponite cakes are also much lower than those for dispersions of spherical particles with the same average radius a, which can be evaluated through the Carman-Kozeny equation:

$$k_p = \frac{(1-\phi)^3}{45\,\phi^2}\,a^2 \qquad (16)$$

If the particle radius a is chosen to give the same mass per particle as that of a Laponite particle, this would yield permeabilities that are 50 times higher than those measured for Laponite sediments. Moreover, the low values of k_p for Laponite sediments are associated with the highly ordered structure of the sediment. Indeed, if divalent cations are added to the original dispersion, the structure becomes completely disordered, and the permeability (at a given volume fraction) rises by a factor of 50, close to the values calculated for spherical particles [27]. Thus, the low permeabilities of ordered Laponite sediments are a consequence of their layered structure, as there the pores that let the water pass across the Laponite layers are extremely small.

With the measured values of the permeabilities, the flux of water through a sediment can be calculated from Darcy's law. If the sediment (thickness s_{max} and area of cross section A) was simply submitted to a pressure difference ΔP, then the flux of water (viscosity μ) would be:

$$Q = \frac{k_p A \Delta P}{s_{\max} \mu} \tag{17}$$

In fact, the sediment exchanges water with a supernatant, under the effect of an osmotic pressure difference Π. Therefore, the swelling is non-uniform, and the flux is non uniform as well. For a first approximation, we ignore these complications, and assume that the flux is uniform across the sediment. Consider an incremental swelling step, where the flux Q causes the sediment volume to increase by $\delta V = A\, ds_{max}$. The time required for this swelling is:

$$\delta t = \frac{\delta V}{Q} = \left(\frac{\mu}{k_p \Pi} \right) \left(s_{\max} \delta s_{\max} \right) \tag{18}$$

At low volume fractions ϕ, the permeability k_p should vary as $k_p \approx \phi^{-2}$, and the osmotic pressure as $\Pi \approx \phi^2$; therefore, the first factor remains constant, and the differential equation can be integrated to give the final height of sediment, which varies as the square root of swelling time. This integration has been performed with the experimental values of permeabilities, osmotic pressures and initial sediment height: it does yield a swelling law where the height of sediment varies as the square root of swelling time; in agreement with the experimental behavior. However, the predicted swelling rate is too low by a constant factor (Figure 11, dashed line). This is an effect of the approximations made in the calculation, since the swelling is non-uniform, and the flux of water does not have to cross the whole sediment height. The comparison with the data indicates that the effective thickness of sediment that is crossed by the swelling flux is 4 times smaller than the total sediment thickness (Figure 11, full line).

After about a month of swelling (square root of swelling time = 5 in Figure 11), there is a second stage where the swelling of the dispersion without added phosphates departs from this law and slows down by a factor of 30. The average volume fraction of the dispersion at this crossover is ϕ = 0.03. This corresponds to the structural transition where the particles flip into aggregated configurations under the effect of edge-face attractions. Accordingly, the reduction in the rate of swelling indicates that the network of aggregates resists swelling. The slowing down is not as marked for the dispersion without phosphates, indicating that the phosphates reduce the life times of edge face or edge-edge contacts.

These considerations explain why swelling (and deswelling) are relatively fast at high volume fractions, because they do not involve any structural reorganization, and much slower at lower volume fractions, where they are limited by structural processes.

Conclusions

During compression or expansion, the state of aqueous Laponite dispersions results from a competition of applied forces and internal forces. Applied forces are osmotic forces that tend to separate the particles from the aqueous phase, e.g. forces that are applied to the boundaries of the particle network, or to individual particles, or to the solvent. Internal forces are of two types: (a), interactions between all electrical charges, including surface charges, edge charges, and all ions in the interstitial solution, and (b), pressures caused by the thermal agitation of the ions.

In general, the competition of all these forces can lead to quite complex behavior. However, the situation becomes rather simple at very high volume fractions ($\phi > 0.03$). Indeed, when the extraction of water pushes the faces of the platelets closer to each other, the cost of overlap of ionic layers becomes prohibitive, so that (b) wins over (a). At this point the particles flip into a parallel configuration, lose their edge-face contact and take regular spacings.

In this simple situation, the internal osmotic pressure is uniquely determined by the spacing: this is the equation of state of the dispersions. In aqueous dispersions made at high volume fractions, it has a power-law behavior that matches the predictions for the force between ionized platelets that are parallel to each other. Equilibrium is reached when the average spacing is such that this internal pressure matches the applied pressure.

Non-equilibrium situations occur when the applied force either exceeds or is below the internal osmotic pressure. In such a situation, water flows out of or into the dispersion, at a rate that is limited by internal friction forces. At high volume fractions, where the particles are parallel to each other, and all voids in the structure have been eliminated, the compression or expansion processes are opposed by hydrodynamic drag forces associated with the permeation of water through the structure. This permeation is quite slow, because the pores that let water pass across the Laponite layers are extremely small. At lower volume fractions, where the particles are aggregated (no longer parallel to each other), permeation is easier, but structural reordering

becomes the limiting process, because the particles may be locked in their configurations by edge-face attractions.

References

1 Rockwood Additives Limited, Moorfield Road Widnes, Cheshire, WA8 0JU, UK.

2 Avery, R.G.; Ramsay, J.D.F. *J. Colloid Interface Sci.* **1986**, *109*, 448.

3 Pignon, F.; Piau, J.M.; Magnin, A. *Phys. Rev. Lett.* **1996**, *76*, 4857.

4 Pignon, F.; Magnin, A.; Piau, J.M. *J. Rheol.* **1996**, *40*, 573

5 Pignon, F.; Magnin, A.; Piau, J.M.; Cabane, B.; Lindner, P.; Diat, O. *Phys. Rev. E* **1997**, *56*, 3281.

6 Cocard, S.; Tassin, J.F.; Nicolaï, T. *J. Rheol.* **2000**, *44*, 585.

7 Martin, C.; Pignon, F.; Magnin, A.; Piau, J.M.; Cabane, B.; Lindner, P. *Phys. Rev. E* **2002**, *66*, 021401.

8 Coussot, P.; Nguyen, Q.D.; Huynh, H.T.; Bonn, D. *J. Rheology* **2002**, *46*, 573.

9 Bonn, D.; Kellay, H.; Tanaka, H.; Wedgam, G.; Meunier, J. *Langmuir* **1999**, *15*, 7534.

10 Levitz, P.; Lécolier, E.; Mourchid, A.; Delville, F.; Lyonnard, S. *Europhys. Lett.* **2000**, *49*, 672.

11 Mongondry, P. *PhD thesis*, Université du Maine – Le Mans – France (**2003**).

12 Mourchid, A.; Delville, F.; Lambard, J.; Lécolier, E.; Levitz, P. Langmuir **1995**, *11*, 1942

13 Mourchid, A.; Lécolier, E.; Van Damme, H.; Levitz, P. Langmuir **1998**, *14*, 4718

14 Qi, Y. *PhD thesis*, Université d'Orléans – France (**1996**).

15 Qi, Y.; Al-Mukhtar, M.; Alcover, J.F.; Bergaya, F. *Appl. Clay Sci.* **1996**, *11*, 185.

16 Alcover, J.F.; Qi, Y.; Al-Mukhtar, M.; Bonnamy, S.; Bergaya, F. *Clay Minerals* **2000**, *35*, 525.

17 Al-Mukhtar, M.; Qi, Y.; Alcover, J.F.; Conard, J.; Bergaya, F. *Clay Minerals* **2000**, ***35***, 537.

18 Gabriel, J.C.P.; Sanchez, C.; Davidson, P, *J. Phys. Chem.* **1996**, *100*, 11139.

19 Lemaire, B.J.; Panine, P.; Gabriel, J.C.P.; Davidson, P. *Europhys. Lett.* **2002**, ***59***, 55.

20 Pignon, F.; Magnin, A.; Piau, J.M.; Cabane, B.; Aimar, P.; Meireles, M.; Lindner, P. *J. Membrane Sci.* **2000**, *174*, 189.

21 Onsager, L. *Ann. N.Y. Acad. Sci.* **1949**, *51*, 627

22 Perdigon-Aller, A.C., Aston, M., Clarke, S.M. *J. Colloid Interface Sci.* **2005**, *290* , 155

23 Neumann, B.S.; Sansom, K.G. *Clay Minerals* **1970**, *8*, 389.

24 Thomson, D.W.; Butterworth, J.T. *J. Colloid Interface Sci.* **1992**, *151* , 236.

25 Sonneville-Aubrun, O.; Bergeron, V.; Gulik-Krzywicki, T.; Jönsson, Bo; Wennerström, H.; Lindner, P.; Cabane, B. *Langmuir* **2000**, *16* 1566

26 Miller, K.T.; Melant, R.M.; Zukoski, C.F. *J. Am. Ceram. Soc.* **1996**, *79* , 2545.

27 Lelièvre, V. *PhD thesis*, INPG, France **2005**.

28 Bonnet-Gonnet, C.; Belloni, L.; Cabane, B. *Langmuir* **1994**, *10*, 4012.

29 Jacrot, B. *Rep. Progr. Phys.* **1976**, *39*, 11

30 Davidson, P.; Levelut, A.M.; Achard, M.F.; Hardouin, F. *Liquid Crystals* **1989**, *5*, 561

31 Davidson, P.; Levelut, A.M. *Liquid Crystals* **1992**, *11*, 469

32 Evans, D.F.; Wennerström, H. "*The colloidal domain*", Wiley-VCH, New York **1994**

33 Jönsson, Bo private communication